

Improving the performance of Tao-Mo non-empirical density functional with broader applicability in quantum chemistry and material sciences

Subrata Jana,^{1,*} Kedar Sharma,² and Prasanjit Samal^{1,†}

¹*School of Physical Sciences, National Institute of Science Education and Research, HBNI, Bhubaneswar 752050, India*

²*School of Physics, Indian Institute of Science Education and Research, Maruthamala, Vithura, Thiruvananthapuram 695551, India*

(Dated: December 4, 2018)

A revised version of the semilocal exchange-correlation functional [Phys. Rev. Lett. 117, 073001 (2016)] (TM) is proposed by incorporating the modifications to its correlation content obtained from the full high-density second-order gradient expansion as proposed in the case of revised Tao-Perdew-Staroverov-Scuseria (revTPSS) [Phys. Rev. Lett. 103, 026403 (2009)] functional. The present construction improves the performance of TM functional over a wide range of quantum chemical and solid-state properties (thermochemistry and structural). More specifically, the cohesive energies, jellium surface exchange-correlation energies, and real metallic surface energies are improved by preserving the accuracy of the solid-state lattice constants and bulk moduli. The present proposition is not only physically motivated but also enhances the applicability of the TM functional. New physical insights with proper exemplification of the present modification which is presented here can further serve for more realistic non-empirical density functional construction.

I. INTRODUCTION

Density functional theory^{1,2} is visualized as an extremely simplified version of the complicated many-electron Schrödinger equation. In this, all the quantum many-electron effects are embedded into an effective one-electron like potential comprising an unknown exchange-correlation (XC) density functional. As the exact analytic form of XC functional is not known. So, the central task of DFT is to approximate the XC energy/potential functional. Several approximations of the XC functionals with broad range of applications in quantum chemistry, solid-state physics, and material sciences are thus proposed^{3–33}. However, due to the reliable, quick and accurate output, the approximate semilocal XC functionals are widely used and the corresponding successes in quantum chemistry and condensed matter physics are undisputed^{34–52}. In fact, approximations of the semilocal exchange-correlation functionals are proposed from various physical viewpoint. In density functional semilocal approximations, there are mainly two classes of approximations that have been widely used. The first one is known as non-empirical or semi-empirical density functional approximations which are practically useful for both the quantum chemists and solid-state physicists. However, heavily parametrized density functionals^{19,20,31} are also proposed but those functionals perform well within the parametrized test set and practically not so stable for the solid-state calculations. There are various ways for constructing the non-empirical density functionals. Some functionals are constructed from constraint satisfaction^{7,15,21–30} or exchange hole model^{18,30} or satisfying both³⁰. Starting from the local density approximation (LDA)³, the higher rungs of XC density functional approximations are constructed by including the gradient of density and incorporating the Kohn-Sham (KS) kinetic energy dependency. The gradient depen-

dent functionals are known as generalized gradient approximations (GGA)^{3–17}. Whereas, those obtained by incorporating the KS kinetic energy functionals as an extra ingredient are recognized as the meta-generalized gradient approximations (meta-GGA)^{18–33}. In this way, developments and subsequent attempt to construct very accurate approximations of XC functionals make DFT as a practically very appealing and widely used theory to extract the wealth of several observable quantities, such as thermochemical and kinematics of molecules, bond lengths and angles, reaction barrier heights, dynamics of molecules, dipole moments, polarizabilities, infrared intensities, lattice constants of solids, bulk moduli, cohesive energies, surface energies etc^{34–52}.

However, recent advances in functional developments and its applications indicate that the desired accuracy of both quantum chemistry and solid-state physics are achievable by satisfying more exact constraints by the non-empirical functionals. One such functional is proposed recently by Tao-Mo³⁰. The motivation of the present work follows from the alluring features of the TM functional. The TM semilocal functional is designed using the density matrix expansion (DME) techniques which are accurate for compact density i.e., atoms and molecules. To perform accurately in the case of solids, the slowly varying fourth-order gradient approximation is also included within the functional form. In the original TM functional, it is shown that the TM exchange performs differently for several solid-state properties with both the TPSS²² and TM correlation energy³⁰ (designed by modifying the TPSS correlation). However, the TM correlation obeys more exact constraint than TPSS for the low-density limit³⁰ and the TM exchange functional coupled with TM correlation performs more accurately than its TMTTPSS counterpart for most of the molecular and solid-state properties^{41,42,45}. Interestingly, for jellium surface XC energy, the TPSS correlation performs better compared to TM correlation⁴⁵. In this work,

we seek a modification to the TM correlation energy prompted by the improvement achieved by the revTPSS correction²³ over TPSS correlation. It's done by implementing the revTPSS like modifications into the correlation energy of the TM functional. It is shown that the modified correlation coupled with TM exchange keeps all the good features of TM functional intact. Additionally, it leads to noticeable improvement of results for most of the thermochemical test sets, cohesive energies, jellium surface XC energies, and surface energies of the real metals by keeping accuracy of lattice constants and bulk moduli. This improvement clearly indicates that the change in correlation energy is necessary to perform equally well for both the thermochemical, bulk and surface properties of solids.

To present all these modifications and functional performances, we organize this paper as follows. In the following section, we will present the underlying physical motivations and relevant modifications to the TM functional. Following it, we will assess the performance of the revised functional thus obtained in the context of thermochemical accuracy, solid-state lattice constants, bulk moduli, cohesive energies, jellium surface XC energies and surface energies of the real metals. We will conclude by discussing the results and future prospects of the proposed revision of the TM functional.

II. THEORY

As our starting point for proposed modification to the TM functional, we consider the TM exchange energy functional having the form³⁰

$$E_{xc} = - \int \rho(\mathbf{r}) \epsilon_x^{unif}(\mathbf{r}) F_x^{TM} d^3r, \quad (1)$$

with ϵ_x^{unif} is the exchange energy density in the uniform electron gas approximation and F_x is the TM exchange enhancement factor³⁰ given by

$$F_x^{TM} = w F_x^{DME} + (1-w) F_x^{sc}. \quad (2)$$

In this the DME based exchange enhancement factor F_x^{DME} is given by $F_x^{DME} = 1/f^2 + 7R/(9f^4)$, with $R = 1 + 595(2\lambda - 1)^2 p/54 - [\tau - 3(\lambda^2 - \lambda + 1/2)(\tau - \tau^{unif} - |\nabla\rho|^2/72\rho)]/\tau^{unif}$ and F_x^{sc} is the slowly varying fourth-order gradient approximation (GE4) which is given by $F_x^{sc} = \{1 + 10[(10/81 + 50p/729)p + 146\tilde{q}^2/2025 - (73\tilde{q}/405)[3\tau_W/(5\tau)](1 - \tau_W/\tau)]\}^{1/10}$, where $\tilde{q} = (9/20)(\alpha - 1) + 2p/3$. In the original construction of TM functional, extrapolation is done between the compact density (i.e, DME) and slowly varying fourth-order density correction (sc) through a function w . As for solids, the slowly-varying bulk valance region is important. Therefore, it is necessary to recover the correct fourth-order density gradient approximation of exchange. The function w is given by,

$$w = \frac{z^2 + 3z^3}{(1 + z^3)^2}, \quad (3)$$

where $z = \frac{\tau^W}{\tau}$ is the meta-GGA ingredient. Due to different behaviors of z , w switches from the molecular or atomic systems to the slowly varying solid-state system i.e., it switches from DME to the slowly varying density limit. It is noteworthy to mention that near the bond center of the molecules, $z \approx 0$ implies that $w \approx 0$. In the core and density tail region, the systems become effectively one or two electron-like i.e., $\tau \approx \tau^W$, which implies $w \approx 1$. In bulk solids, where the semi-classical gradient expansion of the kinetic energy density is valid, $w < 1$. Therefore, for the slowly varying density approximation, both the DME exchange enhancement factor and slowly varying fourth order density gradient expansion contribute.

Regarding the correlation content of the TM functional³⁰, it is based on one-electron self-interaction free TPSS correlation. It includes the modified TPSS correlation satisfying (nearly-) exact constraint in the low-density or strong-interaction limit of meta-GGA correlation³⁰. Also, this modification actually reduces the errors of lattice constant of bulk solids compared to its corresponding TPSS correlation. The modified TM correlation proposed by Tao-Mo is given as follows³⁰,

$$E_c^{TM}[\rho_\uparrow, \rho_\downarrow] = \int d^3r \rho \epsilon_c^{revPKZB} [1 + d \epsilon_c^{revPKZB} (\tau^W/\tau)^3], \quad (4)$$

where

$$\begin{aligned} \epsilon_c^{revPKZB} &= \epsilon_c^{PBE}(\rho_\uparrow, \rho_\downarrow, \nabla\rho_\uparrow, \nabla\rho_\downarrow) [1 + C^{TM}(\zeta, \xi)(\tau^W/\tau)^2] \\ &\quad - [1 + C(\zeta, \xi)](\tau^W/\tau)^2 \sum_\sigma \frac{n_\sigma}{n} \tilde{\epsilon}_c, \end{aligned} \quad (5)$$

with

$$C^{TM}(\zeta, \xi) = \frac{0.1\zeta^2 + 0.32\zeta^4}{\{1 + \xi^2[(1 + \zeta)^{-4/3} + (1 - \zeta)^{-4/3}]/2\}^4} \quad (6)$$

Here, $\zeta = (\rho_\uparrow - \rho_\downarrow)/n$, and $\xi = |\nabla\zeta|/2(3\pi^2\rho)^{1/3}$. The parameter $d = 2.8 \text{ Hartree}^{-1}$ is chosen to accurately predict the jellium surface correlation energy²².

The TM functional is proved to be very accurate in predicting the energetic, and structural properties of atoms, molecules and solids^{41,42,45}. This is due to the exact constraint satisfaction of the exchange hole which is incorporated through F_x^{DME} . This is the first ever functional of its kind which extrapolates between the compact density and slowly varying fourth-order gradient expansion. It is noteworthy to mention that the prime contribution for the atomic and molecular exchange energy comes from the DME exchange term. However, there is still room to improve the performance of the TM functional. The motivation of the present paper follows from the work^{41,42,45}, where it is shown that the TM exchange combined with the TM and TPSS correlations performs differently for the structural and energetic properties of solids. Nevertheless, it is also a common practice to improve the functional performance based on simple

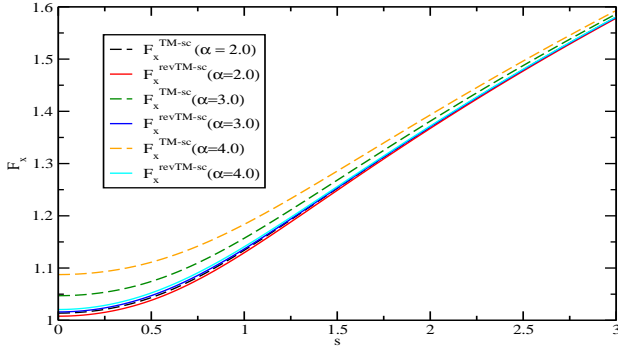


FIG. 1. The slowly varying enhancement factor F_x^{sc} of the TM and revTM functionals with $\alpha = 2.0$, $\alpha = 3.0$, and $\alpha = 4.0$.

modifications on exchange and correlation form. Different modifications based on various physical motivations are done in this direction. For example, based on the Perdew-Kurth-Zupan-Blaha (PKZB)²¹ meta-GGA, the TPSS meta-GGA functional is proposed and later a simple modification on the TPSS exchange and correlation is done through revTPSS²³. Also, we want to acknowledge several works on the recent modifications of the revTPSS and SCAN functional^{24,25,28,32}.

Now, we propose two simple modifications of the TM exchange-correlation functional which improves the molecular, bulk and surface properties of solids keeping all the good properties of the TM functional unalter. In doing so,

(i) we adopt the flexible choice for meta-GGA ingredient \tilde{q} by replacing it with \tilde{q}_b , where $\tilde{q}_b = \frac{9(\alpha-1)}{20[1+b\alpha(\alpha-1)]^{1/2}} + \frac{2p}{3}$. This modification of \tilde{q} is used in TPSS and revTPSS functional but not in TM functional. By construction, \tilde{q}_b becomes \tilde{q} at $b = 0$. Both the \tilde{q}_b and \tilde{q} follow closely the reduced Laplacian gradient (q). For $0 \leq \alpha \leq 1$ (single-orbital towards slowly varying density region⁵²), the $F_x^{revTM-sc}$ (exchange enhancement factor of slowly varying density correction of the revised TM (revTM) functional with \tilde{q}_b) and F_x^{TM-sc} (exchange enhancement factor of slowly varying density correction of the TM functional with \tilde{q}) essentially follow the same behaviour. Whereas, for $\alpha \gg 1$ (regions of overlapping closed shells⁵²) and $s \approx 0$ F_x^{TM-sc} and $F_x^{revTM-sc}$ are quite different which is relevant in the middle of bonds. On the other hand, when α is closer to 1 (slowly varying density region), these enhancement factors are practically the same. In both cases, $F_x^{revTM-sc}$ monotonically increases with the reduced density gradient (s) (shown in Fig. 1). Regarding the parameter b , it is chosen to be 0.40 in TPSS and revTPSS based functional, so that F_x becomes a monotonically increasing function of reduced density gradient (s). However, in our present case, we find no reason to change this value for modification of the TM functional. Therefore, this modification is done in the same spirit as is proposed from the PKZB to TPSS meta-GGA functional.

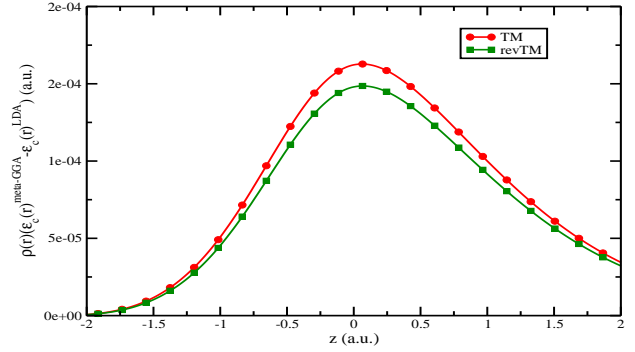


FIG. 2. Difference of the TM and revTM correlation energy

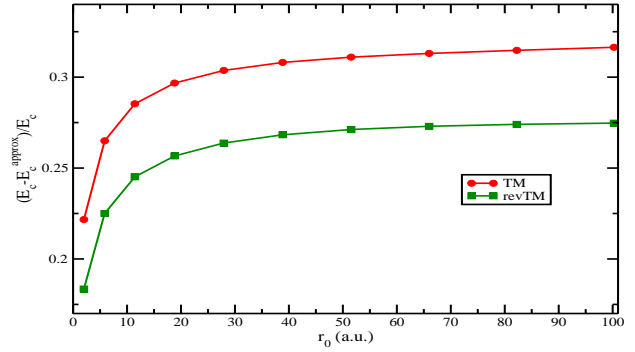


FIG. 3. Error for the correlation energy of the Hooke's atom for the TM and revTM correlation at different values of the classical electron distances $r_0 = (\omega^2/2)^{-1/3}$, where ω is the frequency of the isotropic harmonic potential. Here, E_c is the exact correlation of the Hook's atom.

Having refined the TM exchange, we now focus on the TM correlation. The TM correlation is based on the TPSS correlation, where the parameter $\beta = 0.066725$ is obtained from the high-density limit ($r_s \rightarrow 0$) of the slowly varying second-order gradient approximation of the correlation energy functional. The TPSS correlation, which is based on the PBE correlation adopts the same value of the parameter β . Later, Perdew et.al.²³ adopted a density-dependent β parameter derived by Hu and Langreth⁵³, which correctly recovers the high-density limit ($r_s \rightarrow 0$) of the slowly varying second-order gradient approximation and the low-density limit ($r_s \rightarrow \infty$) of the second-order gradient expansion for exchange (which is 10/81) that cancels the correlation. In our modification of the correlation (ii) we adopt the proposition made by Perdew et.al.²³ in the revTPSS functional and have modified the β^{TPSS} to $\beta^{revTPSS}(r_s) = 0.066725(1+0.1r_s)/(1+0.1778r_s)$, where $r_s = (\frac{3}{4\pi\rho})^{1/3}$ is the Seitz radius. Apart from this modification, we keep the form of the TM correlation intact which is revised from TPSS correlation as³⁰,

$$C(\zeta, 0) = 0.1\zeta^2 + 0.32\zeta^4. \quad (7)$$

This modification is actually necessary to improve the TM correlation energy functional in the low-density limit. Also, as the TM exchange obeys the exact fourth order gradient expansion, the choice of $\beta^{revTPSS}$ in principle can improve the high-density limit of the correlation through the error cancellation between second-order gradient expansion of exchange and correlation. Therefore, modification of the β parameter from the high-density second-order gradient expansion (as is done in TPSS) to the full second-order gradient expansion (which is incorporated in revTPSS) keeps the conditions (i)-(iii) intact for correlation in ref.³⁰ and additionally, in the high-density limit, the second-order gradient terms of the correlation cancels with exchange in the revTM functional.

To complete our analysis, in Fig. 2, we consider the correlation energy densities w.r.t. LDA as a functional of distance (z) of the jellium surface at the bulk parameter $r_s = 2$. Unlike the TM correlation, the revTM correlation slightly de-enhanced inside the bulk solids and in the vacuum. This is logical because the revTM correlation uses the parameter β which is modified from TPSS and the revTM correlation more exactly satisfies the low-density and high density limit^{23,30}. Additionally, in Fig. 3, we show the revTM correlation for the Hooke's atom. This model system is used to predict the functional performance from the low-density or strong-interaction limit (small ω) to the high-density limit (large ω). From Fig. 3, it is evident that the revTM correlation performs better than its TM counterpart due to the satisfaction of more exact constraint. However, more improved β parameter for this type of model system is also proposed in TPSSloc functional²⁴ and later it is used in the BLOC functional²⁵.

III. COMPUTATIONAL DETAILS

To assess the performance of the revTM functional with other popular GGA and meta-GGA functionals, we implement the revTM functional in NWChem⁵⁴ and Vienna Ab initio Simulation Package (VASP)⁵⁵⁻⁵⁸ code for the molecular and solid-state calculations respectively. All molecular and solid-state calculations are done self-consistently using the $6-311++G(3df,3pd)$ basis set in NWChem and plane-wave basis set in VASP. For molecular calculations we consider Minnesota 2.0³⁵ test set which includes (i)AE17 –atomic energies of 17 atoms (H–Cl), (ii) AE6 – atomization energies of 6 molecules, (iii) EA13 - 13 electron affinities, (iv) IP21 – 21 ionization potentials, (v) PA8 – 8 proton affinities, (vi) BH6 – 6 barrier heights, (vii) HB6 – 6 hydrogen bonding, and (viii) DI6 – 6 dipole bonding. Whereas, our solid-state test set contains equilibrium lattice constants (LC29), bulk moduli (BM29), and cohesive energies (COH29) of 29 solids which includes: simple metals (Li, Na, K, Ca, Sr, Ba, Al), transition metals (V, Ni, Cu, Rh, Pd, Ag, Pt), ionic solids (LiF, LiCl, NaF, NaCl, MgO), insulators (BN, BP, AlN), and semiconductors (C, Si, Ge, SiC,

GaN, GaP, GaAs). All the bulk calculations are performed with the $16 \times 16 \times 16$ Γ -centred \mathbf{k} points with energy cutoff 700 eV for the smooth convergence w.r.t. the plane-wave and energy convergence. All solid-state calculations are done considering non-magnetic phases and ambient-condition crystal structures except Ni. For which the magnetic calculations are taken into account. The anti-symmetric box size of $18 \times 19 \times 20 \text{ \AA}^3$ is considered for the atomic calculations.

Besides all these fundamental tests, we also calculate the jellium surface XC energies and surface energies of real metallic systems to incorporate the functional performances. Regarding the surface energy calculations, it is done with $16 \times 16 \times 1$ Γ - centered \mathbf{k} points with energy convergence criterion 1.0×10^{-6} eV and energy cutoff 700 eV. The dipole corrections are also taken into consideration in this calculation along with $> 20 \text{ \AA}$ vacuum to avoid the interaction between the periodic surfaces. The functionals considered for comparison with the revTM are LDA, Perdew-Burke-Ernzerhof (PBE)⁷, PBE reparametrized for solids (PBEsol)¹¹, TPSS²², revTPSS²³, Strongly Constrained and Appropriately Normed (SCAN)²⁹, and TM³⁰. The accuracy in the performance of all the functionals are assessed by calculating mean error (ME), mean absolute error (MAE), and mean absolute relative percentage error (MARPE).

IV. RESULTS

A. Thermochemical accuracy

Let's start with the thermochemical accuracy of each functional. The results of all tests are summarized in Table I, where we report the ME and MAE of the individual test set for each functionals. Inspection of Table I shows that the revised version of TM i.e., revTM performs better than TM for most of the thermochemical test sets. In particular, for AE6, EA13, PA8, HB6 and DI6 test cases, the revTM shows improvement. However, in the atomization energies test sets AE17 and IP13, the performance of TM and revTM qualitatively same. The ME of IP13 is predicted to be much better in revTM than other functionals considered here. In the case of BH6, the TM shows better performance than revTM. It is noteworthy to mention that accurate prediction of barrier heights are quite difficult for semilocal functionals because of the many-electron self-interaction problems in the transition state of those molecules. The range-separated hybrid functionals perform better in such cases because of the proper incorporation of the non-locality information. We also observe that for hydrogen (HB6) and dipole (DI6) bond dissociation energies, the revTM improves the performance of TM. As those are noncovalent interactions and improvement of revTM over TM clearly indicates the change in correlation is important. It is also very interesting observation that, even though the revTPSS

TABLE I. Summary of deviations using different methods in terms of ME and MAE. The least MAE between the TM and revTM are in boldfont.

		L(S)DA	PBE	TPSS	revTPSS	SCAN	TM	revTM
atomic energy (Ha)								
AE17	ME	-0.673	-0.076	0.028	-0.029	-0.220	-0.054	-0.054
	MAE	0.673	0.076	0.028	0.038	0.251	0.054	0.054
atomization energy (kcal/mol)								
AE6	ME	-76.4	-11.8	-3.7	-2.9	-1.1	0.1	-1.1
	MAE	76.4	15.0	5.6	6.0	3.4	5.1	4.3
electron affinity (kcal/mol)								
EA13	ME	-5.60	-1.05	0.76	1.42	1.01	3.20	2.39
	MAE	5.71	2.20	2.37	2.69	3.30	3.72	3.31
ionization potential (kcal/mol)								
IP13	ME	-4.48	-2.01	-1.69	-0.61	-3.80	0.40	-0.01
	MAE	5.31	3.49	3.02	2.91	4.47	2.99	2.98
proton affinity (kcal/mol)								
PA8	ME	4.99	-0.16	-2.81	-2.92	-1.11	-1.60	-1.52
	MAE	4.99	1.42	2.81	2.92	1.20	1.88	1.61
barrier heights (kcal/mol)								
BH6	ME	-17.9	-9.42	-8.34	-7.43	-7.49	-7.45	-7.65
	MAE	17.9	9.42	8.34	7.43	7.49	7.45	7.65
hydrogen bonding (kcal/mol)								
HB6	ME	-4.50	-0.12	0.43	0.40	-0.93	-0.13	0.12
	MAE	4.50	0.32	0.43	0.40	0.93	0.20	0.18
dipole bonding (kcal/mol)								
DI6	ME	-2.92	-0.33	0.35	0.30	-0.60	-0.50	-0.17
	MAE	2.92	0.40	0.51	0.47	1.12	0.50	0.37

correlation does not improve dramatically over the TPSS correlation as far as the thermochemical accuracy is concerned but the change in correlation in the revTM suits perfectly for most of the thermochemical test sets.

Now, concerning the performance of TM based functionals with other meta-GGAs and GGAs, the SCAN performs very well for the AE6 atomization energies. However, we observe that the MAE of revTM for the EA13 matches closely with SCAN for which the PBE performs better than others. For IP13, TPSS, revTPSS, TM and revTM performs similarly. In this case, the SCAN functional gives MAE of 4.47 kcal/mol. In particular, the SCAN functional is quite accurate in case of AE6, PA8, and BH6 test sets. From the improvement of revTM over TM functional, it is quite clear that the change in correlation results to balance description of different thermochemical test sets and thus the change in correlation part in relevant. However, other modifications based on the β parameter are also proposed in the TPSSloc functionals and the resultant functional based on the TPSSloc²⁴ is the BLOC²⁵ functional which also performs quite accurately over an wide range of molecular properties.

B. Solid-state performances

Having established the thermochemical accuracy of the revTM functional, we now focus on the solid-state performance of the functional. Unlike the thermochemical test set, in the present solid-state performance, we include the PBEsol functional which is quite accurate for the solid-state structural properties and its comparison with other functionals is necessary to check the robustness of the functionals performances in a more competitive manner.

Lattice constants : First, we focus on the performance in case of lattice constants. The lattice constant is one of the fundamental properties of solids and the accuracy of several solid-state structural properties depend on the accuracy of obtaining the same. In Table II, we summarize the performances of all the functionals. The zero-point anharmonic expansion (ZPAE) corrected experimental lattice constants values are taken from different literatures and the same are referred in the Table II. In Fig. 4, we also plot the percentage deviation of the different solids given in Table II.

Concerning the overall performance of the relevant

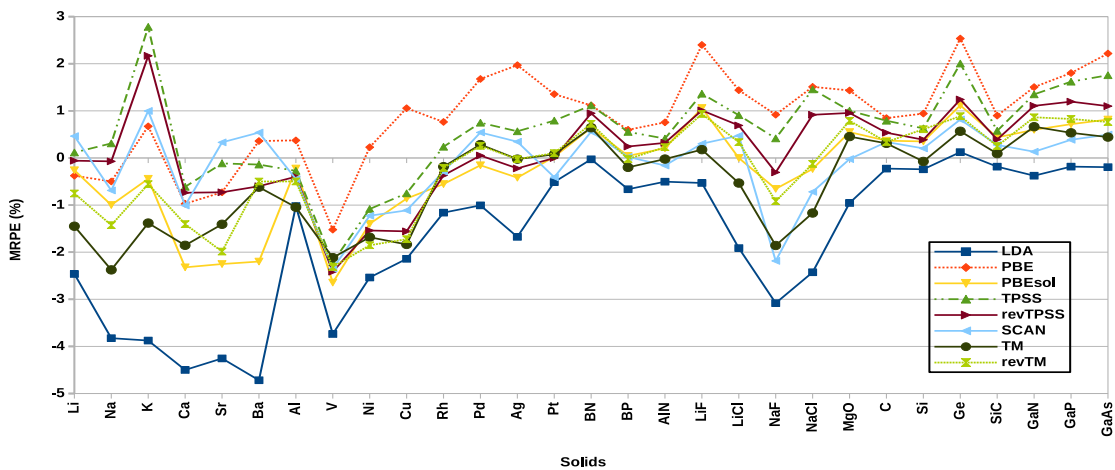


FIG. 4. Shown is the MARE of the lattice constants obtained from different functionals presented in Table II

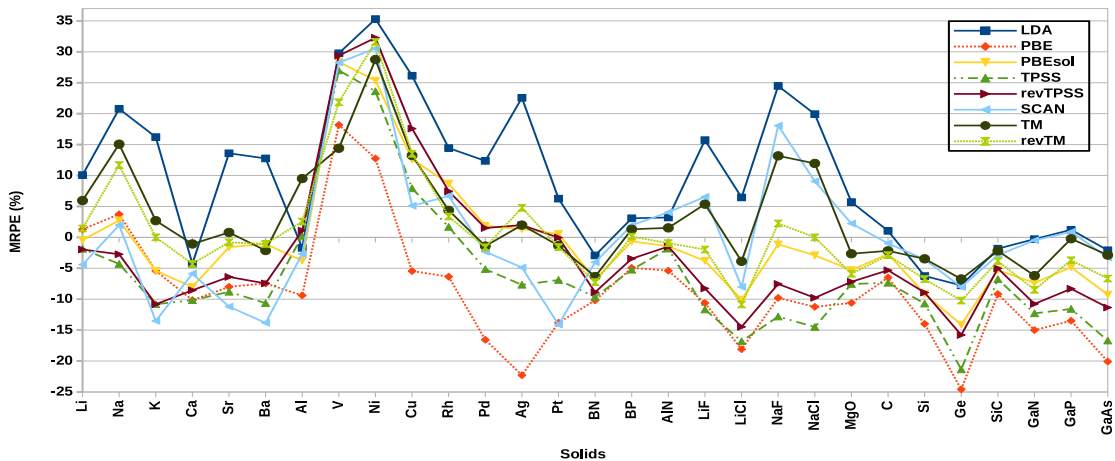


FIG. 5. Shown is the MARE of the bulk moduli of different functionals presented in Table III

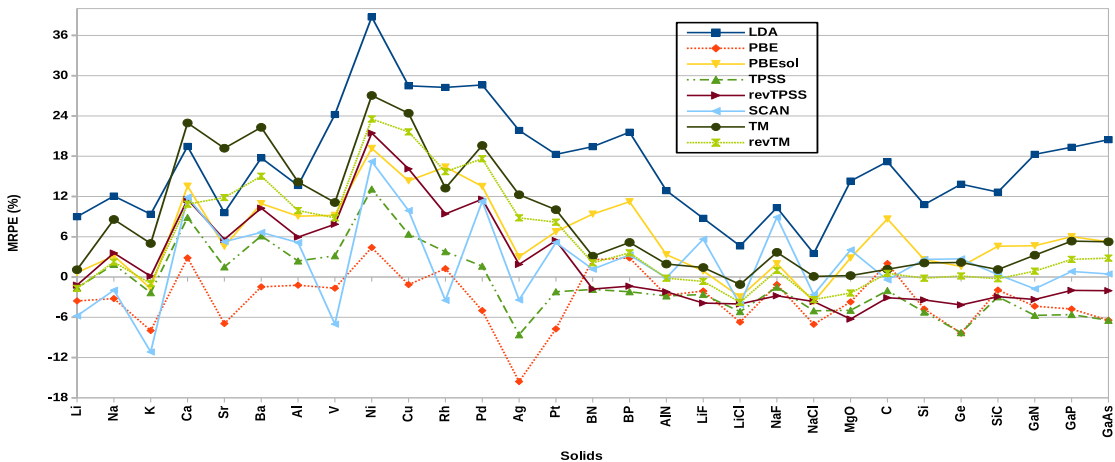


FIG. 6. Shown is the MARE of the cohesive energies of different functionals presented in Table IV

TABLE II. Equilibrium lattice constants (in Å) of different solids are obtained using several functionals considered here. The experimental values (except AlN) are collected from references⁴³, where the correction due to ZPAE is taken into account. The ZPAE corrected AlN reference value is taken from ref.⁵⁹. The best values are in bold and the most deviating values are underlined.

Solids	LDA	PBE	PBEsol	TPSS	revTPSS	SCAN	TM	revTM	Expt.-ZPAE
Simple metals									
Li	<u>3.366</u>	3.438	3.442	3.455	3.449	3.467	3.401	3.425	3.451
Na	<u>4.048</u>	4.188	4.167	4.222	4.206	4.180	4.109	4.149	4.209
K	<u>5.010</u>	5.247	5.189	5.357	5.325	5.264	5.140	5.183	5.212
Ca	<u>5.306</u>	5.502	5.427	5.522	5.515	5.500	5.453	5.478	5.556
Sr	<u>5.783</u>	5.996	5.904	6.033	5.996	6.060	5.955	5.920	6.040
Ba	<u>4.766</u>	5.020	4.892	4.995	4.972	5.029	4.971	4.977	5.002
Al	3.978	4.034	4.010	4.008	4.003	4.001	<u>3.977</u>	3.999	4.019
ME	<u>-0.176</u>	-0.009	-0.065	0.015	-0.003	0.002	-0.069	-0.051	
MAE	<u>0.176</u>	0.029	0.065	0.032	0.036	0.031	0.069	0.051	
MARPE	<u>3.522</u>	0.569	1.242	0.621	0.680	0.640	1.447	1.018	
Transition metals									
V	<u>2.911</u>	2.978	2.944	2.957	2.951	2.953	2.960	2.954	3.024
Ni	<u>3.419</u>	3.516	3.459	3.470	3.454	3.465	3.449	3.443	3.508
Cu	<u>3.519</u>	3.634	3.565	3.569	3.540	3.556	3.530	3.534	3.596
Rh	<u>3.749</u>	3.822	3.772	3.802	3.779	3.782	3.786	3.785	3.793
Pd	3.837	<u>3.941</u>	3.870	3.905	3.878	3.897	3.887	3.886	3.876
Ag	3.994	<u>4.142</u>	4.045	4.085	4.053	4.076	4.061	4.061	4.062
Pt	3.893	<u>3.966</u>	3.914	3.944	3.913	3.897	3.916	3.917	3.913
ME	<u>-0.064</u>	0.032	-0.029	-0.006	-0.029	-0.021	-0.026	-0.027	
MAE	<u>0.064</u>	0.046	0.029	0.032	0.030	0.031	0.030	0.031	
MARPE	<u>1.824</u>	1.224	0.865	0.913	0.879	0.896	0.886	0.927	
Ionic solids									
LiF	3.939	<u>4.055</u>	4.002	4.014	4.000	3.972	3.967	3.997	3.960
LiCl	<u>4.975</u>	5.145	5.072	5.118	5.107	5.096	5.045	5.089	5.072
NaF	<u>4.435</u>	4.618	4.546	4.595	4.562	4.476	4.491	4.534	4.576
NaCl	<u>5.430</u>	5.649	5.552	5.646	5.616	5.525	5.500	5.558	5.565
MgO	4.146	<u>4.246</u>	4.209	4.228	4.226	4.185	4.205	4.219	4.186
ME	<u>-0.087</u>	0.071	0.004	0.048	0.030	-0.021	-0.030	0.008	
MAE	<u>0.087</u>	0.071	0.022	0.048	0.036	0.035	0.041	0.027	
MARPE	<u>1.781</u>	1.540	0.500	1.029	0.776	0.741	0.838	0.620	
Insulators									
BN	3.584	<u>3.625</u>	3.608	3.625	3.619	3.605	3.608	3.611	3.585
BP	<u>4.490</u>	4.547	4.522	4.545	4.531	4.521	4.511	4.519	4.520
AlN	4.346	<u>4.401</u>	4.377	4.386	4.382	4.361	4.367	4.378	4.368
ME	-0.018	<u>0.033</u>	0.011	0.028	0.020	0.005	0.004	0.012	
MAE	0.018	<u>0.033</u>	0.011	0.028	0.020	0.009	0.011	0.012	
MARPE	0.398	<u>0.823</u>	0.297	0.694	0.504	0.247	0.288	0.325	
Semiconductors									
C	3.536	<u>3.574</u>	3.557	3.572	3.563	3.556	3.555	3.556	3.544
Si	5.402	<u>5.466</u>	5.434	5.449	5.436	5.426	5.411	5.448	5.415
Ge	5.646	<u>5.782</u>	5.702	5.752	5.709	5.685	5.671	5.689	5.639
SiC	4.332	<u>4.379</u>	4.359	4.365	4.357	4.352	4.344	4.351	4.340
GaN	4.503	<u>4.588</u>	4.547	4.581	4.570	4.526	4.550	4.559	4.520
GaP	5.425	<u>5.533</u>	5.474	5.523	5.500	5.456	5.464	5.480	5.435
GaAs	5.626	<u>5.762</u>	5.683	5.736	5.699	5.665	5.662	5.680	5.637
ME	-0.009	<u>0.079</u>	0.032	0.064	0.043	0.019	0.018	0.033	
MAE	0.011	<u>0.079</u>	0.032	0.064	0.043	0.019	0.019	0.033	
MARPE	0.219	<u>1.535</u>	0.629	1.246	0.851	0.379	0.384	0.649	
TME	<u>-0.089</u>	0.040	-0.013	0.029	0.010	-0.003	-0.023	-0.008	
TMAE	<u>0.089</u>	0.053	0.036	0.042	0.034	0.027	0.037	0.034	
TMARPE	<u>1.952</u>	1.154	0.778	0.920	0.768	0.615	0.830	0.767	

TABLE III. Bulk moduli (in GPa) of different solids are obtained using concerned functionals. The experimental values are taken from ref.^{44,47,50,59}. The best values are in bold and the most deviating values are underlined.

Solids	LDA	PBE	PBEsol	TPSS	revTPSS	SCAN	TM	revTM	Expt.
Simple metals									
Li	<u>15.3</u>	14.1	13.8	13.6	13.6	13.3	14.7	14.1	13.9
Na	<u>9.3</u>	8.0	7.9	7.4	7.5	7.9	8.9	8.6	7.7
K	<u>4.3</u>	3.5	3.5	3.3	3.3	3.2	3.8	3.7	3.7
Ca	17.9	16.8	17.2	<u>16.8</u>	17.1	17.6	18.5	17.9	18.7
Sr	<u>14.2</u>	11.5	12.3	11.4	11.7	11.1	12.6	12.4	12.5
Ba	10.6	8.7	9.3	8.4	8.7	<u>8.1</u>	9.2	9.3	9.4
Al	80.6	74.3	78.9	82.2	82.9	79.8	<u>89.8</u>	84.1	82.0
ME	0.6	<u>-1.6</u>	-0.7	-0.7	-0.4	-1.0	1.4	0.3	
MAE	1.2	<u>1.7</u>	0.8	0.7	0.7	1.0	1.5	0.6	
MARPE	<u>11.3</u>	6.5	3.3	6.7	5.6	7.6	5.3	3.1	
Transition metals									
V	<u>206.2</u>	187.8	204.0	201.8	205.6	203.8	181.8	193.6	158.9
Ni	<u>250.3</u>	208.6	231.9	228.7	244.7	241.5	238.2	243.5	185.0
Cu	<u>182.9</u>	137.1	163.3	156.5	170.5	152.4	164.2	164.6	145.0
Rh	<u>311.4</u>	254.8	295.8	276.7	292.4	290.3	284.0	281.3	272.1
Pd	<u>222.6</u>	<u>165.3</u>	201.8	187.9	201.1	193.5	195.3	194.9	198.1
Ag	<u>135.8</u>	86.1	112.3	102.3	113.0	105.4	113.0	116.1	110.8
Pt	302.0	245.0	285.8	264.6	284.1	<u>244.1</u>	280.4	279.7	284.2
ME	<u>36.7</u>	-9.9	20.1	9.2	22.5	11.0	14.7	17.1	
MAE	<u>36.7</u>	24.9	20.1	20.1	22.5	25.3	16.6	19.3	
MARPE	<u>21.0</u>	13.6	11.3	11.4	12.9	13.1	9.4	11.2	
Ionic solids									
LiF	<u>88.3</u>	68.2	73.4	67.4	70.0	81.3	80.4	74.8	76.3
LiCl	41.2	<u>31.7</u>	34.8	32.2	33.1	35.6	37.2	34.5	38.7
NaF	<u>66.1</u>	47.9	52.5	46.3	49.1	62.7	60.1	54.3	53.1
NaCl	<u>33.1</u>	24.5	26.8	23.6	24.9	30.1	30.9	27.6	27.6
MgO	179.5	<u>151.8</u>	160.8	157.0	157.6	173.6	165.3	159.8	169.8
ME	<u>8.5</u>	-8.3	-3.4	-7.8	-6.2	3.6	1.7	-2.9	
MAE	<u>8.5</u>	8.3	3.4	7.8	6.2	4.8	4.1	3.4	
MARPE	<u>14.5</u>	12.1	4.6	12.7	9.4	8.8	7.4	4.2	
Insulators									
BN	398.2	<u>368.4</u>	382.1	370.7	373.8	393.7	384.2	380.5	410.2
BP	173.2	159.7	166.9	<u>159.2</u>	162.2	171.3	170.2	168.2	168.0
AlN	208.5	<u>191.1</u>	199.1	198.3	199.0	210.2	205.1	200.1	202.0
ME	-0.1	<u>-20.3</u>	-10.7	-17.3	-15.1	-1.7	-6.9	-10.5	
MAE	7.9	<u>20.3</u>	10.7	17.3	15.1	9.3	10.4	10.6	
MARPE	3.1	<u>6.8</u>	3.0	5.6	4.6	3.3	3.1	2.8	
Semiconductors									
C	459.5	425.2	442.5	<u>421.3</u>	430.5	450.3	444.8	441.6	454.7
Si	94.5	<u>86.7</u>	91.6	90.0	91.8	97.2	97.3	94.0	100.8
Ge	71.3	<u>58.3</u>	66.4	60.8	65.1	71.1	72.1	69.4	77.3
SiC	224.9	<u>208.1</u>	217.0	213.6	217.6	222.5	224.1	220.3	229.1
GaN	209.4	<u>178.5</u>	194.5	184.2	187.4	209.0	197.0	192.2	210.0
GaP	90.1	<u>77.0</u>	84.7	78.7	81.6	89.8	88.8	85.7	89.0
GaAs	75.1	<u>61.3</u>	69.6	63.9	68.0	74.2	74.5	71.6	76.7
ME	-1.8	<u>-20.4</u>	-10.2	-17.9	-13.7	-3.4	-5.6	-9.0	
MAE	3.5	<u>20.4</u>	10.2	17.9	13.7	3.6	5.6	9.0	
MARPE	2.9	<u>14.7</u>	7.5	12.4	9.4	2.9	3.4	6.1	
TME	10.0	<u>-11.2</u>	0.5	-5.4	-0.6	2.0	2.1	0.5	
TMAE	12.3	<u>14.9</u>	9.2	12.5	11.5	9.0	7.5	8.6	
TMARPE	<u>11.3</u>	11.2	6.4	10.1	8.8	7.6	6.0	5.9	

functionals, as usual, the LDA functional underestimates the lattice constants, whereas PBE overestimates the lattice constants. The overestimation of the PBE functional is reduced by restoring the exact second-order gradient correction as applied in the PBEsol functional. Regarding the meta-GGA functionals, the TPSS functional

overestimates the lattice constants which is improved by the revised version of the TPSS i.e., revTPSS. As mentioned earlier, the revTPSS functional has been proposed by modifying the exchange enhancement factor such that the slowly varying density gradient approximation is satisfied for an wide range of the reduced density gradient

TABLE IV. Cohesive energies (in eV/atom) of different solids are obtained using different functionals. The experimental values are taken from ref.^{44,47,50,59}. The best values are in bold and the most deviating values are underlined.

Solids	LDA	PBE	PBEsol	TPSS	revTPSS	SCAN	TM	revTM	Expt.
Simple metals									
Li	<u>1.807</u>	1.599	1.669	1.631	1.638	1.562	1.676	1.630	1.658
Na	<u>1.254</u>	1.083	1.154	1.140	1.159	1.097	1.215	1.144	1.119
K	<u>1.028</u>	0.865	0.924	0.918	0.941	<u>0.835</u>	0.987	0.931	0.940
Ca	2.222	1.913	2.112	2.025	2.075	<u>2.081</u>	<u>2.287</u>	2.062	1.860
Sr	1.896	1.610	1.809	1.756	1.827	1.821	<u>2.062</u>	1.935	1.730
Ba	2.249	1.882	2.119	2.027	2.106	2.037	<u>2.336</u>	2.197	1.910
Al	3.899	3.389	3.742	3.513	3.635	3.607	<u>3.917</u>	3.771	3.431
ME	0.244	-0.044	0.126	0.052	0.105	0.056	<u>0.262</u>	0.146	
MAE	0.244	0.059	0.130	0.066	0.110	0.120	<u>0.262</u>	0.157	
MARPE	12.980	3.890	6.231	3.534	5.466	6.835	<u>13.326</u>	7.504	
Transition metals									
V	<u>6.633</u>	5.251	5.831	5.509	5.760	4.965	5.933	5.811	5.340
Ni	<u>6.216</u>	4.677	5.339	5.067	5.441	5.251	5.692	5.535	4.480
Cu	<u>4.528</u>	3.484	4.029	3.749	4.092	3.873	4.384	4.286	3.524
Rh	<u>7.417</u>	5.855	6.731	6.001	6.327	5.582	6.549	6.691	5.783
Pd	<u>5.065</u>	3.741	4.470	4.002	4.395	4.383	4.710	4.632	3.938
Ag	<u>3.637</u>	2.520	3.075	2.728	3.041	2.883	3.351	3.248	2.985
Pt	<u>6.943</u>	5.416	6.267	5.741	6.189	6.172	6.459	6.350	5.870
ME	<u>1.217</u>	-0.139	0.546	0.125	0.475	0.170	0.737	0.662	
MAE	<u>1.217</u>	0.216	0.546	0.236	0.475	0.364	0.737	0.662	
MARPE	<u>26.921</u>	5.251	11.769	5.551	10.537	8.211	16.815	14.901	
Ionic solids									
LiF	<u>4.847</u>	4.364	4.497	4.341	4.284	4.708	4.520	4.428	4.457
LiCl	<u>3.752</u>	<u>3.345</u>	3.480	3.401	3.442	3.439	3.546	3.451	3.586
NaF	<u>4.381</u>	3.925	4.049	3.910	3.859	4.324	4.116	4.009	3.970
NaCl	<u>3.454</u>	<u>3.102</u>	3.214	3.169	3.215	3.249	3.340	3.225	3.337
MgO	<u>5.947</u>	<u>5.010</u>	5.351	4.945	4.877	5.413	5.214	5.079	5.203
ME	<u>0.366</u>	-0.161	0.008	-0.157	-0.175	0.116	0.037	-0.072	
MAE	<u>0.366</u>	0.161	0.099	0.157	0.175	0.210	0.053	0.088	
MARPE	<u>8.308</u>	4.138	2.475	3.853	4.123	5.064	1.302	2.227	
Insulators									
BN	<u>8.073</u>	6.934	7.394	6.635	6.639	6.839	6.970	6.903	6.760
BP	<u>6.249</u>	5.286	5.717	5.027	5.070	5.309	5.405	5.325	5.140
AlN	<u>6.603</u>	5.691	6.045	5.685	5.721	5.844	5.963	5.840	5.850
ME	<u>1.058</u>	0.054	0.469	-0.134	-0.107	0.081	0.196	0.106	
MAE	<u>1.058</u>	0.160	0.469	0.134	0.107	0.085	0.196	0.113	
MARPE	<u>17.957</u>	2.711	7.979	2.289	1.786	1.520	3.398	1.962	
Semiconductors									
C	<u>8.842</u>	7.697	8.198	7.392	7.312	7.513	7.632	7.586	7.545
Si	<u>5.191</u>	4.461	4.806	4.440	4.525	4.808	4.783	4.677	4.685
Ge	<u>4.460</u>	3.590	3.980	3.593	3.755	4.024	4.003	3.924	3.918
SiC	<u>7.298</u>	6.352	6.775	6.287	6.288	6.501	6.550	6.461	6.478
GaN	<u>5.382</u>	4.352	4.762	4.290	4.398	4.470	4.698	4.590	4.550
GaP	<u>4.308</u>	3.438	3.827	3.408	3.538	3.640	3.803	3.705	3.610
GaAs	<u>4.020</u>	3.122	3.512	3.122	3.269	3.352	3.512	3.431	3.337
ME	<u>0.768</u>	-0.159	0.248	-0.227	-0.148	0.026	0.123	0.036	
MAE	<u>0.768</u>	0.202	0.248	0.227	0.148	0.058	0.123	0.043	
MARPE	<u>16.082</u>	4.667	4.760	5.179	2.996	1.307	2.910	1.065	
TME	<u>0.711</u>	-0.105	0.272	-0.053	0.063	0.089	0.297	0.202	
TMAE	<u>0.711</u>	0.160	0.289	0.169	0.218	0.176	0.300	0.235	
TMARPE	<u>16.803</u>	4.327	6.746	4.344	5.481	4.978	8.554	6.252	

(s). Also, modification in the correlation energy functional is incorporated in order to take care the full linear response. Regarding the most advanced meta-GGA functionals, the SCAN improves the meta-GGA performance and results the least MAE. Concerning the overall performances of TM and revTM functionals, the revTM

slightly improves the performance of TM.

Now, we focus on the performance of TM and revTM for the individual group of solid-state structures as mentioned in Table II. For the simple metals and ionic insulators, we observe a clear improvement in the lattice constants by revTM functional. The TM functional only per-

forms better than revTM for the semiconductors. However, for transition metals, and insulators both TM and revTM performs almost equivalently. The systematic improvement in the performances of the revTM can be understood as the change in the correlation functional and the change of $\tilde{q} \rightarrow \tilde{q}_b$ which slightly reduces the effect of exchange enhancement factor. More physically, in the intershell region (where α may be larger even for small s (as shown in Fig. 1)), the F_x^{TM-sc} enhances the exchange energy density. Thus, the exchange hole becomes more centered in the intershell region than the outer shell region which effects in the reduction in the lattice constants. On the other hand, the modification of $\tilde{q} \rightarrow \tilde{q}_b$ in revTM functional actually reduces this effect and shows extension in the lattice constants. This is clearly evident from Table II, where we observe that the lattice constants obtained using revTM functional for simple metals, and ionic solids extend little bit compared to its TM functional counterpart. Therefore, we can say that this small modification in the exchange enhancement factor quite reasonably improves the lattice constants of those solids for which TM has the tendency to underestimate the lattice constants slightly. Concerning the correlation effect, the full linear response β affects the lattice constants by cancelling the error of exchange and correlation in the low-density limit. However, we observe a PBEsol like tendency in the performance of revTM. Note that in the alkali metals and ionic solids, the long-range van der Waals interaction between the semi-core states shrink the lattice constants, which is correctly captured by the SCAN, TM and revTM functionals because SCAN includes the intermediate vdW interaction and TM based functionals include the long-range vdW interaction due to the oscillation of the exchange hole. However, slight elongation in the revTM is observed compared to TM because the revTM exchange enhancement factor is now de-enhanced than TM in the density overlap region as shown in Fig. 1. Through the modifications of TM functional we observe small but systematic improvement in the lattice constants of revTM over TM.

Bulk moduli : The accuracy of bulk moduli depends on the accuracy of the lattice constants. The performance of functionals for the bulk moduli are presented in Table III and MRPE is plotted in Fig. 5. Here, we use third order Birch-Murnaghan equation of state to fit the energy-volume curve. Regarding the overall performances, the TM functional gives the least MAE followed by the revTM and SCAN functionals. The revTM improves the performance of TM functional for simple metals and ionic solids. This is because the lattice constants of the revTM functionals are obtained to be better for those solids. For the very same reason, the semiconductor bulk moduli are underestimated by revTM compared to the TM functional. Concerning the performance of other functionals, the tendency in the lattice constants is followed in the performance of bulk moduli. Except the SCAN and TM based functionals, other GGA and meta-GGA functionals show underestimation in results

for most of the solids. Most pronounced underestimation is observed for PBE functional, while the LDA, as usual, overestimates the bulk moduli and shows tendency opposite to that of PBE.

Cohesive energies: Next, we assess the performance of revTM along with other functionals for the cohesive energies of solids. The performance of functionals are presented in Table IV and plotted in Fig. 6. Here, also we observe interesting performance for revTM compared to TM functionals as the revTM improves the performance over TM for most of the solids. Individual consideration shows that the revTM improves the performance for simple metals, transition metals, insulators, and semiconductors. For ionic solids, the performance of TM is slightly better than revTM. This is quite natural because the change in correlation energy in revTM actually suits more than TM correlation and cancels error for second-order gradient approximation with correlation for the low-density limit. We observe that for most of the solids, the revTM reduces the cohesive energies of the TM. Therefore, improves the overall performance of the cohesive energies. However, within meta-GGA functionals, the least MAE is observed using the TPSS functional. Also, the SCAN functional is quite good in predicting the cohesive energies compared to TM and revTM. The SCAN functional suits better for the simple metals, transition metals, and insulators in comparison to the revTM. Regarding the GGA based functionals. As usual, the PBE performs better compared to the PBEsol. This is due to the improved atomization energies of PBE compared to the PBEsol.

V. REAL METALLIC SURFACE ENERGIES

Investigating any new XC functional performance for the real metallic surfaces are particularly interesting because those analysis has industrial applications. Several meta-GGA are developed along the Jacob ladder with increasing accuracy in metal surface energy. Recent progress in this direction shows that the non-local functional SCAN+rVV10⁵¹ (SCAN functional plus revised Vydrov-van Voorhis non-local correlation functional) and quasi 2D-GGA functionals¹⁷ predict the most accurate metallic surface energies. However, in this work we assess the metallic surface energies of the semilocal XC functionals without including any non-local correlation. The main aim of this paper is to assess the accuracy of LDA, PBE, PBEsol TPSS, revTPSS, SCAN, TM, and revTM functional for the metal surface energies. However, in our comparison we do not include the SCAN+rVV10 results and to the best of our knowledge, the comparison of SCAN and TM functionals for the real metallic surfaces are done for the first time in this paper.

But before going into the real application of the metallic surface energies, we consider the surface exchange-correlation energy of the jellium model¹³. The jellium serves as a model for the metallic systems. It consists of

TABLE V. The jellium surface exchange-correlation energies (σ_{xc}) (in erg/cm²) of different functionals. The LDA, PBE, PBEsol, revTPSS values are taken from ref.²³. The SCAN values are taken from ref.⁵¹. The DMC values are taken from ref.⁵¹. Rest of the functional values are calculated in this work.

r_s	σ_{xc}^{LDA}	σ_{xc}^{PBE}	σ_{xc}^{PBEsol}	σ_{xc}^{TPSS}	$\sigma_{xc}^{revTPSS}$	σ_{xc}^{SCAN}	σ_{xc}^{TM}	σ_{xc}^{revTM}	DMC
2	3354	3265	3374	3380	3428	3422	3517	3468	3392±50
3	764	741	774	772	783	788	824	803	768±10
4	261	252	267	266	268	274	291	280	261±8
6	53.0	52.0	56.7	55.5	55.4	58.9	64.7	60.3	53.0
ME	-10.5	-41.0	-0.6	-0.1	15.1	17.2	55.7	34.3	
MAE	10.5	41.0	8.4	5.9	15.1	17.2	55.7	34.3	
MARE	0.4	3.1	2.6	1.9	2.5	4.9	11.1	6.9	

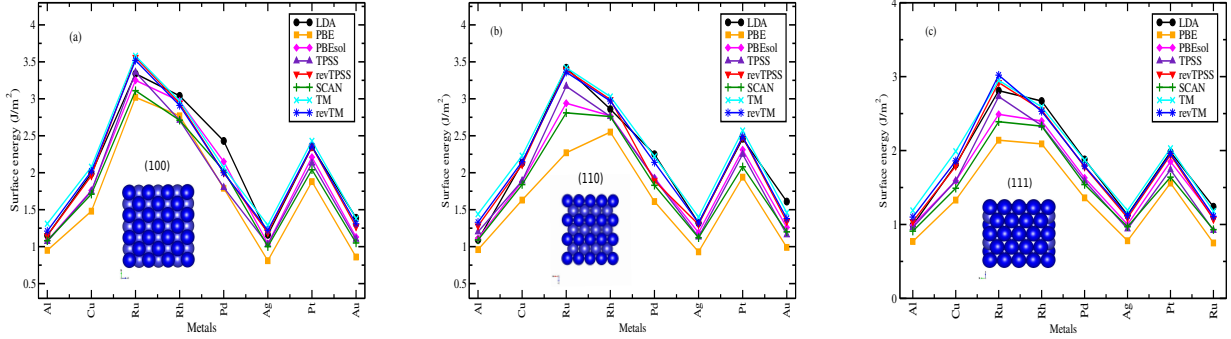


FIG. 7. Shown are the surface energies (J/m²) for the selected metals using different functionals.

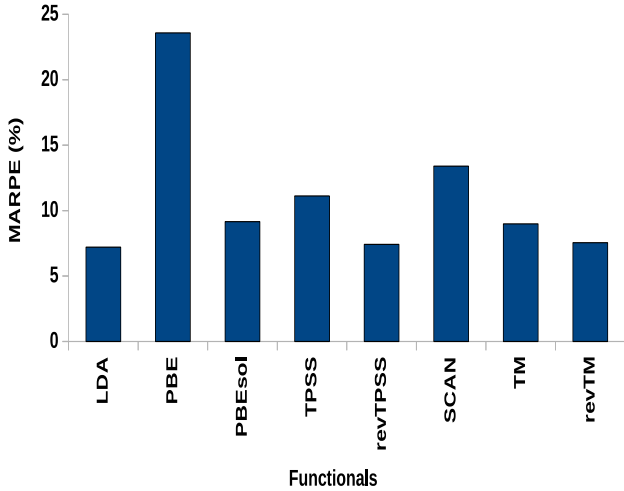


FIG. 8. Shown are the total MARPE of different functionals calculated using mean surface energies for selected metals.

a homogeneous electron gas, where the electron charges are compensated with the positive background charge. The bulk density of the jellium model remains constant

and varies rapidly on the surface. Because in solids the valence electron density is slowly varying, the analysis of jellium surface XC energies helps to understand the accuracy of a particular XC energy for the solid-state systems. The underlying jellium surface exchange-correlation energy is defined as¹³,

$$\sigma_{xc} = \int_{-\infty}^{\infty} dz \rho(z) [\epsilon_{xc}[\rho; z] - \epsilon_{xc}^{unif}[\bar{\rho}]]. \quad (8)$$

In Table V, we present the jellium surface XC energies of the functionals under consideration. In this case, the diffusion Monte Carlo (DMC) results are considered as the reference values. An interesting observation is that the revTM reduces the jellium surface XC energies of the TM functional and predicts the values close to the DMC values. However, for these simple jellium systems, the LDA, GGA and other meta-GGA functionals are also quite accurate. The improvement in the jellium surface energies is well-known fact from the change in correlation as it is already mentioned in revTPSS paper²³. In their work, it is mentioned that the reduction of β with r_s actually decreases surface energies which in fact reflects in the performance of the revTM functional. Therefore, the change in the correlation is important and well suited with the TM functional.

As a real test and assessment of the revTM functional,

TABLE VI. Metallic surface energy (J/m^2) computed using the considered functionals. The LDA, PBE, PBEsol, and SCAN functionals results and reference values are taken from ref.⁵¹. The best values are in bold and the most deviating values are underlined.

Metals	Surfaces	LDA	PBE	PBEsol	TPSS	revTPSS	SCAN	TM	revTM	Expt.
Al	100	1.15	0.95	1.08	1.07	1.15	1.08	1.31	1.21	
	110	1.09	0.96	1.11	1.20	1.28	1.09	1.44	1.33	
	111	0.99	0.77	0.99	0.96	1.04	0.91	1.19	1.10	
	$\bar{\sigma}$	1.08	<u>0.89</u>	1.06	1.08	1.16	1.03	1.31	1.21	1.14
Cu	100	1.99	1.48	1.76	1.75	1.96	1.71	2.08	2.02	
	110	2.13	1.63	1.88	1.89	2.11	1.84	2.23	2.15	
	111	1.81	1.33	1.59	1.59	1.79	1.49	1.99	1.86	
	$\bar{\sigma}$	1.98	<u>1.48</u>	1.74	1.74	1.95	1.68	<u>2.10</u>	2.01	1.79
Ru	100	3.34	3.02	3.25	3.36	3.56	3.11	3.58	3.52	
	110	3.42	2.27	2.94	3.17	3.39	2.81	3.42	3.36	
	111	2.81	2.14	2.49	2.73	2.92	2.39	2.95	3.02	
	$\bar{\sigma}$	3.19	<u>2.48</u>	2.89	3.09	3.29	2.77	3.32	3.30	3.04
Rh	100	3.04	2.77	2.97	2.71	2.94	2.71	2.97	2.91	
	110	2.86	2.55	2.77	2.76	2.99	2.76	3.03	2.97	
	111	2.67	2.09	2.40	2.34	2.55	2.33	2.59	2.53	
	$\bar{\sigma}$	<u>2.86</u>	2.47	2.71	2.60	2.83	2.60	2.86	2.80	2.66
Pd	100	2.43	1.79	2.15	1.80	2.00	2.03	2.07	2.00	
	110	2.25	1.61	1.93	1.92	1.89	1.83	2.22	2.14	
	111	1.88	1.36	1.63	1.59	1.78	1.54	1.87	1.79	
	$\bar{\sigma}$	2.19	<u>1.59</u>	1.90	1.77	1.97	1.80	2.05	1.98	2.00
Ag	100	1.16	0.81	1.04	1.03	1.19	1.00	1.29	1.22	
	110	1.32	0.93	1.19	1.13	1.30	1.12	1.40	1.32	
	111	1.13	0.78	1.00	0.94	1.09	0.97	1.19	1.12	
	$\bar{\sigma}$	1.20	<u>0.84</u>	1.08	1.03	1.19	1.03	1.29	1.22	1.25
Pt	100	2.35	1.88	2.21	2.13	2.35	2.04	2.43	2.36	
	110	2.46	1.94	2.31	2.25	2.48	2.08	2.57	2.49	
	111	1.98	1.56	1.85	1.74	1.94	1.64	2.03	1.96	
	$\bar{\sigma}$	2.26	<u>1.79</u>	2.12	2.04	2.26	1.92	2.34	2.27	2.49
Au	100	1.39	0.86	1.13	1.10	1.27	1.05	1.38	1.31	
	110	1.61	0.99	1.26	1.16	1.34	1.20	1.46	1.38	
	111	1.24	0.75	1.10	0.92	1.07	0.93	1.18	1.11	
	$\bar{\sigma}$	1.41	<u>0.87</u>	1.16	1.06	1.23	1.06	1.34	1.27	1.51
ME (J/m^2)		0.04	<u>-0.43</u>	-0.15	-0.18	0.00	-0.25	0.09	0.02	
MAE (J/m^2)		0.15	<u>0.43</u>	0.17	0.20	0.15	0.25	0.17	0.15	
MARPE (%)		7.21	<u>23.58</u>	9.16	11.12	7.42	13.40	8.99	7.55	

we consider the surface energies of the real metals compiled in ref⁵¹. It is defined as the energy required to construct a surface from an infinite crystal. Computationally, it is measured by the formula,

$$\sigma = \frac{1}{2A} \left(E_N^{slab} - N \epsilon_{atom}^{bulk} \right), \quad (9)$$

where E_N^{slab} is the total energy of the relaxed surface slab with N atoms, and ϵ_{atom}^{bulk} is energy of the bulk with one atom and A is the slab surface area.

In practice, it is suggested to measure the mean of all surfaces to compare with the experimental surface energies. Therefore, we compare the surface energies taking the mean of the contribution of the values obtained from (100), (110), and (111) surfaces. In Table VI, we sum-

marize the contribution of each surface energies. Here, the LDA, PBE, PBEsol, and SCAN values are taken from ref.⁵¹. The TPSS, revTPSS, TM, and revTM surface energies are calculated in this work. In Fig. 7 and Fig. 8, we plot the surface energy contribution from each surface and MARPE respectively. Investigation of the contribution of the surface energies obtained from different surfaces using semilocal functionals, we remark that LDA gives quality surface energies due to the well-known cancellation of error in exchange and correlation. The PBE underestimates the surface energies due to the inability of the recovering the exact second-order gradient approximation which indeed necessary for the good surface energies. By recovering the exact second-order gradient approximation, the PBEsol improves the perfor-

mance over PBE. While improving the correlation and more conveniently obeying the fourth-order gradient approximations over a broader range of density gradient approximations, the revTPSS improves the surface energies over TPSS. For the very same reason (as applied in the correlation) we observe the improvement in the surface energies for revTM over TM functional. Overall consideration shows that the LDA, revTPSS, and revTM functional agree very well with the experimental values. Interesting observation is that the TM functional overestimates the surface energies for most of the metals which are actually corrected by its revTM counterpart.

VI. CONCLUSIONS

In this work, we proposed a revised TM (revTM) functional by improving the slowly varying density correction of the exchange and incorporating the revTPSS like correlation energy in the functional form. The proposed modification over TM functional is assessed for the solid-state lattice constants, bulk moduli, cohesive energies, jellium surface exchange-correlation energies and surface energies of the metals. Performance of the revTM functional shows its accuracy over broad range of the molecular and solid-state systems. Specifically, it improves the cohesive energies, jellium surface energy-correlation energies, surface energies of real metals and molecular atomization energies by maintaining the overall accuracy of the lattice constants and bulk moduli. As the physical insight of the revTM functional performances, one can say that both the molecular and solid-state systems are treated in a more balanced way because it works well both for the localized (e.g., AE6 atomization energies) and delocalized systems (solid-state physics). It's because the density matrix expansion based exchange hole is localized by nature and proper incorporation of the slowly varying fourth-order gradient expansion. The

present modification keeps all the good properties of the TM functional, additionally, it improves the functional performances in the low-density limit through a simple revision. It is also noticed that the present modifications treat both the quantum chemical and solid-state properties in a more balanced way than other accurate and widely appreciated meta-GGA like SCAN functional.

As a concluding remark, we can say that the revTPSS and revTM have one thing in common i.e. both cancel exchange and correlation at the low-density limit. However, the construction of the TM exchange functional is different from those constructed only from the fourth-order gradient approximation. In the case of TM exchange functional, part of the exchange hole is constructed from density matrix expansion which is more localized than the convenient exchange hole obtained from the fourth-order gradient approximation. Therefore, it is desirable to cancel the error in the low-density ($r_s \rightarrow \infty$) limit when the more localized density matrix expansion based exchange hole is coupled with the exchange hole of the fourth-order gradient approximation which indeed holds in the revTM functional. However, more conventionally and quite physically motivated β form can also be derived for the TM exchange functional which is a matter of our future study.

VII. ACKNOWLEDGEMENT

S.J. and P.S. would like to acknowledge and thank Dr. Lucian A. Constantin for providing some computational resources and useful comments regarding the work. S.J. would also like to acknowledge the financial support from the Department of Atomic Energy, The government of India. K.S. would like to acknowledge the financial support from the Department of Science and Technology, Government of India, during his summer internship in NISER under the supervision of P.S..

* subrata.jana@niser.ac.in

† psamal@niser.ac.in

¹ P. Hohenberg and W. Kohn, Phys. Rev. **136**, B864 (1964).

² W. Kohn and L. J. Sham, Phys. Rev. **140**, A1133 (1965).

³ J. P. Perdew and A. Zunger, Phys. Rev. B **23**, 5048 (1981).

⁴ A. D. Becke, Phys. Rev. A **38**, 3098 (1988).

⁵ C. Lee, W. Yang, and R. G. Parr, Phys. Rev. B **37**, 785 (1988).

⁶ J. P. Perdew, J. A. Chevary, S. H. Vosko, K. A. Jackson, M. R. Pederson, D. J. Singh, and C. Fiolhais, Phys. Rev. B **46**, 6671 (1992).

⁷ J. P. Perdew, K. Burke, and M. Ernzerhof, Phys. Rev. Lett. **77**, 3865 (1996).

⁸ R. Armiento and A. E. Mattsson, Phys. Rev. B **72**, 085108 (2005).

⁹ Z. Wu and R. E. Cohen, Phys. Rev. B **73**, 235116 (2006).

¹⁰ Y. Zhao and D. G. Truhlar, The Journal of Chemical Physics **128**, 184109 (2008), <https://doi.org/10.1063/1.2912068>.

¹¹ J. P. Perdew, A. Ruzsinszky, G. I. Csonka, O. A. Vydrov, G. E. Scuseria, L. A. Constantin, X. Zhou, and K. Burke, Phys. Rev. Lett. **100**, 136406 (2008).

¹² L. A. Constantin, J. P. Perdew, and J. M. Pitarke, Phys. Rev. B **79**, 075126 (2009).

¹³ L. A. Constantin, L. Chiodo, E. Fabiano, I. Bodrenko, and F. D. Sala, Phys. Rev. B **84**, 045126 (2011).

¹⁴ E. Fabiano, L. A. Constantin, and F. Della Sala, Journal of Chemical Theory and Computation **7**, 3548 (2011), pMID: 26598253, <https://doi.org/10.1021/ct200510s>.

¹⁵ L. A. Constantin, A. Terentjevs, F. Della Sala, P. Cortona, and E. Fabiano, Phys. Rev. B **93**, 045126 (2016).

¹⁶ A. Cancio, G. P. Chen, B. T. Krull, and K. Burke, The Journal of Chemical Physics **149**, 084116 (2018), <https://doi.org/10.1063/1.5021597>.

- ¹⁷ L. Chiodo, L. A. Constantin, E. Fabiano, and F. Della Sala, *Phys. Rev. Lett.* **108**, 126402 (2012).
- ¹⁸ A. D. Becke and M. R. Roussel, *Phys. Rev. A* **39**, 3761 (1989).
- ¹⁹ T. Van Voorhis and G. E. Scuseria, *The Journal of Chemical Physics* **109**, 400 (1998), <https://doi.org/10.1063/1.476577>.
- ²⁰ Y. Zhao and D. G. Truhlar, *The Journal of Chemical Physics* **125**, 194101 (2006), <https://doi.org/10.1063/1.2370993>.
- ²¹ J. P. Perdew, S. Kurth, A. c. v. Zupan, and P. Blaha, *Phys. Rev. Lett.* **82**, 2544 (1999).
- ²² J. Tao, J. P. Perdew, V. N. Staroverov, and G. E. Scuseria, *Phys. Rev. Lett.* **91**, 146401 (2003).
- ²³ J. P. Perdew, A. Ruzsinszky, G. I. Csonka, L. A. Constantin, and J. Sun, *Phys. Rev. Lett.* **103**, 026403 (2009).
- ²⁴ L. A. Constantin, E. Fabiano, and F. D. Sala, *Phys. Rev. B* **86**, 035130 (2012).
- ²⁵ L. A. Constantin, E. Fabiano, and F. Della Sala, *Journal of Chemical Theory and Computation* **9**, 2256 (2013), pMID: 26583719, <https://doi.org/10.1021/ct400148r>.
- ²⁶ J. Sun, R. Haunschild, B. Xiao, I. W. Bulik, G. E. Scuseria, and J. P. Perdew, *The Journal of Chemical Physics* **138**, 044113 (2013), <https://doi.org/10.1063/1.4789414>.
- ²⁷ J. Sun, J. P. Perdew, and A. Ruzsinszky, *Proceedings of the National Academy of Sciences* **112**, 685 (2015), <http://www.pnas.org/content/112/3/685.full.pdf>.
- ²⁸ A. Ruzsinszky, J. Sun, B. Xiao, and G. I. Csonka, *Journal of Chemical Theory and Computation* **8**, 2078 (2012), pMID: 26593840, <https://doi.org/10.1021/ct300269u>.
- ²⁹ J. Sun, A. Ruzsinszky, and J. P. Perdew, *Phys. Rev. Lett.* **115**, 036402 (2015).
- ³⁰ J. Tao and Y. Mo, *Phys. Rev. Lett.* **117**, 073001 (2016).
- ³¹ Y. Wang, X. Jin, H. S. Yu, D. G. Truhlar, and X. He, *Proceedings of the National Academy of Sciences* **114**, 8487 (2017), <http://www.pnas.org/content/114/32/8487.full.pdf>.
- ³² P. D. Mezei, G. I. Csonka, and M. Kllay, *Journal of Chemical Theory and Computation* **14**, 2469 (2018), pMID: 29565589, <https://doi.org/10.1021/acs.jctc.8b00072>.
- ³³ F. Della Sala, E. Fabiano, and L. A. Constantin, *International Journal of Quantum Chemistry* **116**, 1641, <https://onlinelibrary.wiley.com/doi/pdf/10.1002/qua.25224>.
- ³⁴ C. J. Cramer and D. G. Truhlar, *Phys. Chem. Chem. Phys.* **11**, 10757 (2009).
- ³⁵ R. Peverati and D. G. Truhlar, *Philosophical Transactions of the Royal Society of London A: Mathematical, Physical and Engineering Sciences* **372** (2014), <http://rsta.royalsocietypublishing.org/content/372/2011/20120476.full.pdf>.
- ³⁶ V. N. Staroverov, G. E. Scuseria, J. Tao, and J. P. Perdew, *The Journal of Chemical Physics* **119**, 12129 (2003), <https://doi.org/10.1063/1.1626543>.
- ³⁷ Y. Zhao, N. E. Schultz, and D. G. Truhlar, *Journal of Chemical Theory and Computation* **2**, 364 (2006), pMID: 26626525, <https://doi.org/10.1021/ct0502763>.
- ³⁸ L. Goerigk and S. Grimme, *Journal of Chemical Theory and Computation* **7**, 291 (2011), pMID: 26596152, <https://doi.org/10.1021/ct100466k>.
- ³⁹ P. Hao, J. Sun, B. Xiao, A. Ruzsinszky, G. I. Csonka, J. Tao, S. Glindmeyer, and J. P. Perdew, *Journal of Chemical Theory and Computation* **9**, 355 (2013), pMID: 26589038, <https://doi.org/10.1021/ct300868x>.
- ⁴⁰ L. Goerigk, A. Hansen, C. Bauer, S. Ehrlich, A. Najibi, and S. Grimme, *Phys. Chem. Chem. Phys.* **19**, 32184 (2017).
- ⁴¹ Y. Mo, G. Tian, R. Car, V. N. Staroverov, G. E. Scuseria, and J. Tao, *The Journal of Chemical Physics* **145**, 234306 (2016), <https://doi.org/10.1063/1.4971853>.
- ⁴² Y. Mo, G. Tian, and J. Tao, *Phys. Chem. Chem. Phys.* **19**, 21707 (2017).
- ⁴³ P. Haas, F. Tran, and P. Blaha, *Phys. Rev. B* **79**, 085104 (2009).
- ⁴⁴ F. Tran, J. Stelzl, and P. Blaha, *The Journal of Chemical Physics* **144**, 204120 (2016), <https://doi.org/10.1063/1.4948636>.
- ⁴⁵ Y. Mo, R. Car, V. N. Staroverov, G. E. Scuseria, and J. Tao, *Phys. Rev. B* **95**, 035118 (2017).
- ⁴⁶ A. E. Mattsson, R. Armiento, J. Paier, G. Kresse, J. M. Wills, and T. R. Mattsson, *The Journal of Chemical Physics* **128**, 084714 (2008), <https://doi.org/10.1063/1.2835596>.
- ⁴⁷ J. Sun, M. Marsman, G. I. Csonka, A. Ruzsinszky, P. Hao, Y.-S. Kim, G. Kresse, and J. P. Perdew, *Phys. Rev. B* **84**, 035117 (2011).
- ⁴⁸ G. I. Csonka, J. P. Perdew, A. Ruzsinszky, P. H. T. Philipsen, S. Lebègue, J. Paier, O. A. Vydrov, and J. G. Ángyán, *Phys. Rev. B* **79**, 155107 (2009).
- ⁴⁹ S. Jana, A. Patra, and P. Samal, *The Journal of Chemical Physics* **149**, 044120 (2018), <https://doi.org/10.1063/1.5040786>.
- ⁵⁰ S. Jana, K. Sharma, and P. Samal, *The Journal of Chemical Physics* **149**, 164703 (2018), <https://doi.org/10.1063/1.5047863>.
- ⁵¹ A. Patra, J. E. Bates, J. Sun, and J. P. Perdew, *Proceedings of the National Academy of Sciences* **114**, E9188 (2017), <http://www.pnas.org/content/114/44/E9188.full.pdf>.
- ⁵² J. Sun, B. Xiao, Y. Fang, R. Haunschild, P. Hao, A. Ruzsinszky, G. I. Csonka, G. E. Scuseria, and J. P. Perdew, *Phys. Rev. Lett.* **111**, 106401 (2013).
- ⁵³ C. D. Hu and D. C. Langreth, *Phys. Rev. B* **33**, 943 (1986).
- ⁵⁴ M. Valiev, E. Bylaska, N. Govind, K. Kowalski, T. Straatsma, H. V. Dam, D. Wang, J. Nieplocha, P. P. Zhang, W. W. Liu, and G. L. Milne, *Computational Physics Communications* **181**, 1477 (2010).
- ⁵⁵ G. Kresse and J. Hafner, *Phys. Rev. B* **47**, 558 (1993).
- ⁵⁶ G. Kresse and J. Furthmüller, *Phys. Rev. B* **54**, 11169 (1996).
- ⁵⁷ G. Kresse and D. Joubert, *Phys. Rev. B* **59**, 1758 (1999).
- ⁵⁸ G. Kresse and J. Furthmüller, *Computational Materials Science* **6**, 15 (1996).
- ⁵⁹ J. Harl, L. Schimka, and G. Kresse, *Phys. Rev. B* **81**, 115126 (2010).